博 士 論 文

FUSION OF RAW 264.7 MACROPHAGE CELLS ON MICRO-SCALE FINE PILLAR PATTERNS

(マイクロスケールパターン上における RAW264.7 細胞の融合)

平成 31 年 3 月申請

北海道大学

大学院歯学研究科口腔医学専攻

本　間　淳

FUSION OF RAW 264.7 MACROPHAGE CELLS ON MICRO-SCALE FINE PILLAR PATTERNS

J. HONMA[a], T. AKASAKA[b*], M. TAMAI[b], Y. YOSHIMURA[c], T. TAIRA[d], H. MIYAJI[e], S. YAMAGATA[a], Y. SATO[a], Y. YOSHIDA[b]

[a] *Department of Orthodontics, Faculty of Dental Medicine and Graduate School of Dental Medicine, Hokkaido University, Sapporo 060-8586, Japan*
[b] *Department of Biomaterials and Bioengineering, Faculty of Dental Medicine, Hokkaido University, Sapporo 060-8586, Japan*
[c] *Department of Molecular Cell Pharmacology, Faculty of Dental Medicine and Graduate School of Dental Medicine, Hokkaido University, Kita-ku, Sapporo 060-8586, Japan*
[d] *Cosmo Bio Co., Ltd., Sapporo Division, 3-513-2, Zenibako, Otaru Hokkaido 047-0261, Japan*
[e] *Department of Periodontology and Endodontology, Faculty of Dental Medicine, Hokkaido University, Sapporo 060-8586, Japan*

* Corresponding author: akasaka@den.hokudai.ac.jp
Tsukasa AKASAKA
Tel.: +81 706 4250; fax: +81 706 4251.

Macrophage-dependent immune response to the implant surface sometimes results in failure of implant. Macrophage behaviors are sensitive to the topological factors involving micro/nano-patterns on the implant surface. However, further investigations about macrophage behaviors toward the fine micro/nano-patterns on the implant surface are required. In the present study, we investigated the effects of fine micro-scale pillar patterns found on the surface of implants on macrophage fusion. Micropillars with diameters of 2 μm, 1 μm, and 500 nm and a height of 500 nm were fabricated by nanoimprinting on a cyclo-olefin polymer (COP) film. RAW 264.7 macrophages attachment assay shows that 1 μm- and 500 nm-pillars improved cell attachment than the planar surface. Macrophage fusion assay shows that the number of multinucleated cells on 1 μm- and 500 nm-pillars was approximately 1.4 to 1.5 times higher than that on the planar surface. However, 2 μm-pillar was ineffective in both the assays. Interestingly, the expression of F-actin and vinculin in mononuclear and multinucleated

cells on the pillars appeared ring shaped along the circumference of pillars, indicating frustrated phagocytosis. We suggest that fine micro-patterning of the substrate could be one of the factors that control cell attachment and fusion of RAW 264.7 cells.

Keywords: Cell attachment; macrophage fusion; micro-pattern; pillar-pattern; RAW 264.7.

1. Introduction

Dental implants have been widely used for replacing missing teeth. Various types of dental implants have been developed [1, 2]. The surface topographies of implants are modified with smooth and rough materials to give machined, porous, or patterned at micro- or nano-level. Interestingly, the different topographies express different cell responses at the biomaterial-tissue interaction [3]. Macrophages play a key role in immunity and foreign body reaction [4]. In foreign-body reaction, macrophages develop contacts with the implant surface and exhibit fibrous encapsulation. Then, they release oxygen radicals and degradative enzymes. Moreover, macrophages undergo fusion to generate multinucleated giant cells (MNGCs) including as the foreign-body giant cells (FBGCs) [5] that display remarkable pro-inflammatory or wound-healing capacities. The foreign body reaction by the macrophages, thereby provokes a chronic inflammatory response at the surface of the implant which may sometimes result in failure of implant.

In respect of topography, macrophages exhibit preferred attachment to the rough surfaces compared to the smoother ones both *in vitro* [6] and *in vivo* [7]. Furthermore, macrophage fusion is also affected by micro- and nano-scale roughness of the surface [8, 9]. In the previous studies, Moon et al. reported that epoxy micro-grooves increased fusion of RAW 264.7 cells to form multinucleated cells compared to the corresponding planar surface *in vitro* [10]. Lamers et al. reported that titanium-coated nano-grooves increased macrophage fusion *in vivo* [11]. On the other hand, Chen et al. reported that poly(s-caprolactone) create grooves of widths 500 nm and 2 μm that reduce macrophage fusion *in vivo* [12]. Padmanabhan et al. reported that bulk metallic glass nanorod array reduced the macrophage fusion compared to corresponding planar surface [13]. Further, Wang et al. reported that metallic glass micro-pillar patterns induced greater macrophage fusion, but the nano-pillars restricted the area of macrophage fusion [14]. These data indicate that the macrophage fusion is

sensitive to the topological features and chemical composition of implant surface. Although macrophage fusion on fine micro/nano-grooves [11, 12], nano-rods [13], titania nanotube [15], and metallic glass pillar [14] has been studied, further investigations about macrophage fusion on micro/nano-scale fine patterns at the implant surface are required.

In the present study, we investigated the effect of fine micro-scale pillar patterns on macrophage fusion. Micropillars with diameters of 2 μm, 1 μm, and 500 nm and a height of 500 nm were fabricated by nanoimprinting of a cyclo-olefin polymer (COP) film for basic topological study for application to the dental implants. RAW 264.7 macrophage cells were used to estimate cell attachment and fusion behavior on the pillars. We demonstrate that 1 μm or 500 nm-pillar patterning increase the cell attachment and macrophage fusion.

2. Materials and Methods

2.1. Preparation of the COP pillar-patterned film

COP pillar pattern was fabricated as reported previously [16]. The silicon master mold containing holes with 5 × 5 mm^2 area of holes and diameters of 2 μm, 1 μm, or 500 nm and a depth of 500 nm was purchased from Kyodo International, Inc. (Kawasaki, Japan). Replicas of the master mold were prepared by pressing a COP film (ZF14-188, 188 μm thickness, ZEON Corp., Tokyo, Japan) onto the master mold using a heating press (175 °C, 2 MPa, 4 min). The resulting film was peeled off from the mold. Before performing the biological assays, the film was exposed to low-pressure air plasma in a plasma generator device (YHS-R; Sakigake-Semiconductor Co., Ltd., Kyoto, Japan) for 4 sec. For stabilization of plasma-treated surface, the film was maintained in the air for 1 week. The patterned film was fixed on a 3.5-cm or 6-cm tissue culture dish and sterilized under UV irradiation for 6 min.

For scanning electron microscopy (SEM; S-4000; Hitachi High-Tech Fielding Co.) observations, the surface of patterned film was coated with Pt-Pd using an ion-sputtering device (E-1030; Hitachi High-Tech Fielding Co., Tokyo, Japan) [16].

2.2. Cell attachment assay

To estimate cell attachment on the pillar-patterned film, an assay was performed using murine monocyte/macrophage cell line RAW 264.7 (ATCC no. TIB-71TM, USA) as described previously [17]. The stored RAW 264.7 macrophages

were cultured at 37 °C in a humidified 5% CO_2 atmosphere in Dulbecco's modified Eagle's medium (DMEM; Sigma-Aldrich, St. Louis, MO, USA) containing 10% fetal bovine serum (FBS; CELLect™ Silver; MP Biomedicals, Santa Ana, CA, USA) and 1% penicillin-streptomycin-amphotericin B suspension (Wako Pure Chemical Industries, Ltd., Osaka, Japan). The cells were collected by scraping and seeded at a density of 50,000 cells/cm^2 of the pillar-patterned film. After 1 h, the cells were rinsed with phosphate-buffered saline (PBS), fixed with 2.5% glutaraldehyde solution and stained with Giemsa dye. The numbers of attached cells were counted from 10.7 mm^2 random fields in the optical microscope images. Values represent the mean and standard deviation of the number of the cells on five specimens of each pattern.

2.3. Macrophage fusion assay

To estimate macrophage fusion on the pillar-patterned films, we carried out a multinucleation assay using RAW 264.7 macrophages, using previously reported protocol with a few modifications [15, 17]. The stored RAW 264.7 cells were cultured in DMEM containing 10% FBS for 1 day. The cells were collected by scraping and seeded at a density of 6,000 cells/cm^2 of the pillars. The cells were cultured at 37 °C in a humidified 5% CO_2 atmosphere in α-minimum essential medium (α-MEM; Gibco, Grand Island, NY, USA) containing 10% FBS, and 1% penicillin-streptomycin-amphotericin B suspension. The culture medium was changed every 2 days. After 6 days, the cells were fixed with 2.5% glutaraldehyde solution and stained with Giemsa dye. The numbers of multinucleated cells were counted for each patterned film in 35.7 mm^2 fields from optical microscope images. The cells with > 3 nuclei were counted as multinucleated cells. Values represent the mean and standard deviation of the number of the cells on five specimens of each pattern.

For functional characterizations of macrophages, the cells were subjected to tartrate-resistant acid phosphatase (TRAP) staining [8, 17-19]. Briefly, the cells cultured for 6 days were fixed and stained using a TRAP staining kit (Cosmo Bio Co., Ltd., Tokyo, Japan) according to manufacturer's instructions. After washing with deionized water, the nuclei were stained with 30 µl of 4',6-diamidino-2-phenylindole (DAPI) solution (1 mg/ml; Dojindo Laboratories, Kumamoto, Japan) in 2 mL of deionized water at 37 °C for 1 h. Finally, the cells were washed three times in deionized water and mounted with ProLong® Diamond antifade mounting reagent (Thermo Fisher Scientific Inc., Tokyo, Japan) and observed under a digital microscope (BZ-9000; Keyence Corp., Osaka, Japan). The red colored TRAP image was acquired under visible mode and the blue fluorescence image of DAPI was acquired under fluorescence mode of the

microscope.

2.4. SEM observation of the cells

For SEM observation [17], the cells on the pillar-patterned films were rinsed with PBS, fixed with 2.5% glutaraldehyde solution, and then dehydrated in a series of alcohol solutions (50%, 60%, 70%, 80%, 90%, 95%, 99.5%, and 100%) followed by critical-point drying. The dried cells on the films were coated by Pt-Pd sputtering and observed under SEM.

2.5. Immunofluorescence

Immunofluorescence staining of the cells was performed as described previously [20, 21]. Briefly, after 6 days incubation, the cells were washed three times in PBS and fixed for 5 min in 4% paraformaldehyde in PBS. The cells were then permeabilized with 0.5% Triton X-100 in PBS for 10 min followed by three washings with PBS and blocked in 1% bovine serum albumin (BSA) for 30 min. After washing with PBS, the cells were incubated with 6 µl of anti-vinculin Alexafluor® 488 (0.5 mg/ml; eBioscience, San diego, CA, USA), 3 µl of Acti-stain™ 555 fluorescent phalloidin (14 µM; Cytoskeleton Inc., Denver, CO, USA), and 3 µl of DAPI solution (1 mg/ml; Dojindo Laboratories, Kumamoto, Japan) in 500 µl of PBS containing 1% BSA at 37 °C for 1 h followed by an overnight incubation at 4 °C. Finally, the stained cells were washed thrice in PBS, mounted using ProLong® Diamond antifade mounting reagent (Thermo Fisher Scientific Inc., Tokyo, Japan), and observed under fluorescence microscope (BZ-9000; Keyence Corp., Osaka, Japan).

2.6. Statistical analysis

Statistical analysis was performed using GraphPad Prism version 6.04 (GraphPad Software, Inc., La Jolla, CA, USA). All the data are presented as mean ± standard deviation (n = 5). Statistical differences were assessed by one-way ANOVA with Tukey's multiple comparison post-hoc tests. A p value < 0.05 indicated statistical significance.

3. Results and discussion

3.1. Preparation of the COP pillar-patterned film

To evaluate the cell attachment and fusion assays of RAW 264.7 macrophages

(Fig. 1a), we patterned the COP films via thermal nanoimprinting. The advantage of the COP film for thermal nanoimprinting is its precision molding ability [22-24]. The degree of wettability of COP films can be easily modified from low to high by plasma treatment. Furthermore, COP films are non-toxic and stable in cell culture medium. Thus, COP films were selected for the assays of RAW 264.7 cells. We prepared the COP pillar-patterned films using quartz mold with holes of 2 µm, 1 µm, and 500 nm diameters and 500 nm depth. SEM image shows the fine shape of the pillars according to the corresponding fine shape of the hole in the quartz mold (Fig. 1b).

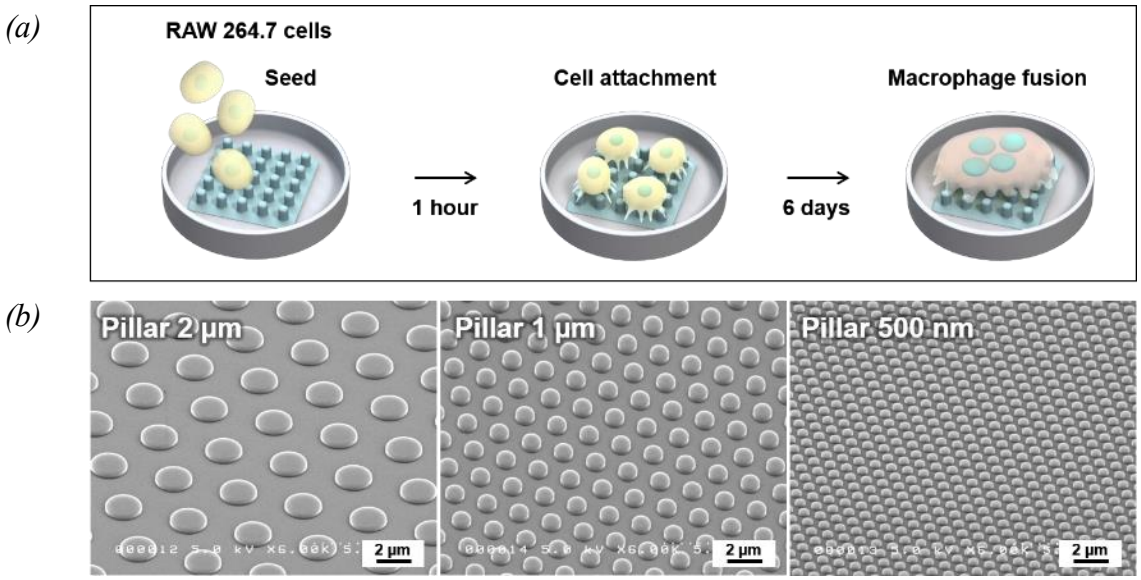

Fig. 1. (a) Illustration of cell attachment and macrophage fusion assays of RAW 264.7 cells on cyclo-olefin polymer (COP) pillar-patterned film. (b) SEM images of the surface of COP pillar-patterned films with diameters of 2 µm, 1 µm, and 500 nm and a height of 500 nm at a 45 ° tilt angle.

3.2. Cell attachment on COP pillar-patterned films

Figure 2a shows representative SEM images of RAW 264.7 cells attached on COP pillar-patterned film. The morphology of attached cells was similar amongst the pillar-patterned and planar surface. The cells on both the films exhibited a round shape with extended filopodia. Some filopodia from the cell body helped in grasping the pillar shape. The round shape of RAW 264.7 cells on our pillar pattern is similar to the morphology of RAW 264.7 cells observed on the G-PET hole pattern with a diameter and depth of 500 nm [17]. By contrast, the round shape of the RAW 264.7 cells on the pillar pattern was different from spindle shape of the cells observed on

micro/nano-groove patterns [11, 25]. The morphology of the cells on patterns was largely affected by the shape of the patterns. Figure 2b shows the number of attached RAW 264.7 cells on the pillars after 1 h of incubation. The average number of attached cells on the pillars with diameters of 1 μm and 500 nm was approximately 1.1 to 1.2 times higher than that on the planar surface ($p < 0.05$). There was not significantly difference in the average number of cells attached on the planar surface and those on the pillar pattern with a diameter of 2 μm ($p > 0.05$). Increased attachment of RAW 264.7 cells by pillar patterning compared with the corresponding planar surfaces conforms with the increased attachment of murine macrophages on the silica micro-grooves with widths of 2 μm and 10 μm [26] and RAW 264.7 cells on the titania nanotube with a diameter of 73 nm [15]. By contrast, a decreased attachment resulting from patterning was observed for polycaprolactone/poly(lactic-*co*-glycolic acid) grooves with widths of 15 μm and 20 μm using RAW 264.7 cells [25]. Ineffective attachment of RAW 264.7 macrophages was observed by patterning for poly(dimethyl siloxane) grooves with widths from 250 nm to 2 μm [12] and chitosan pillars with diameters of 170 nm and 300 nm [27]. The attachment of RAW 264.7 cells might be affected by several factors such as the size and shape of the patterns, and the surface chemical composition. In this study, the COP pillars with diameters of 1 μm and 500 nm probably induced higher cell attachment due to the hook effect of the pillars. However, the pillar-pattern did not produce any difference in the cell spreading compared to the corresponding planar surface at an early stage of cell culturing.

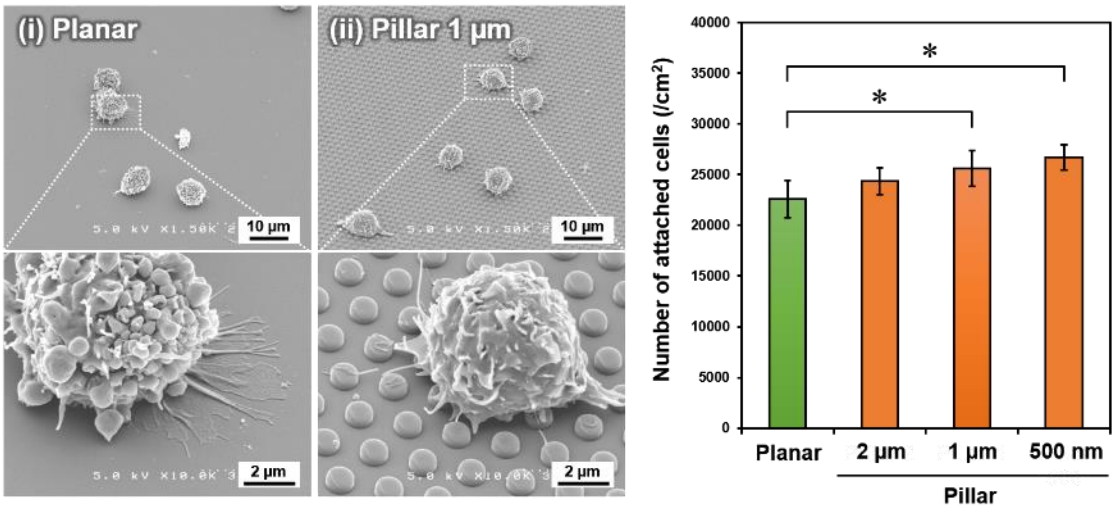

(a) *(b)*

Fig. 2. Assay of attachment of RAW 264.7 cells to cyclo-olefin polymer (COP) pillar films following 1 hour-incubation. (a) Representative SEM images of the cells (i) on the

*corresponding planar surface and (ii) on the surface of pillar film with a diameter of 1 μm and a height of 500 nm at a 45 ° tilt angle. Dotted square area was magnified and shown in the images below. (b) Bar graph showing the number of attached RAW 264.7 cells on the pillar-patterned films with diameters of 2 μm, 1 μm, and 500 nm and a height of 500 nm after 1 hour. * indicates $p < 0.05$.*

3.3. Macrophage fusion assay

Figure 3 shows the fusion of RAW 264.7 cells to form multinucleated cells on COP pillar-patterned films with diameters of 2 μm, 1 μm, and 500 nm and a height of 500 nm after 6 days of culturing. Although a large number of mononuclear RAW 264.7 cells were observed, a small number of multinucleated cells (probably FBGCs) were also observed on both the planar surface and pillar pattern. Fusion of macrophages results in the formation of multinucleated cells [4, 5, 28]. The morphology of multinucleated cells on both the surfaces was similar as observed under optical microscope after 6 days-culturing. Figure 3b shows the number of multinucleated cells with > 3 nuclei on the COP pillar-patterned films and planar surface. The patterning of the COP film significantly affects the efficiency of fusion of RAW 264.7 macrophages. The average numbers of multinucleated cells on the pillars with diameters of 1 μm and 500 nm were approximately 1.4 to 1.5 times higher than those on the planar surface ($p < 0.05$). The average number of multinucleated cells on pillars with a diameter of 2 μm was lesser compared to that on the planar surface, although the difference was not significant ($p > 0.05$). The finding of increase in the numbers of multinucleated cells on the patterned films compared to those on the planar surface is in agreement with the reported increase in the number of multinucleated cells observed on Ti-coated grooves with 150 nm to 1 μm width [11]. Furthermore, the increasing tendency of macrophages to form multinucleated cells by patterning was also observed on plasma-treated epoxy grooves with 100 nm to 1 μm roughness [10]. They suggest that the difference in the tendency of macrophage fusion on patterns and planar surface depends on the difference in protein adsorption on the two surfaces. In contrast, decrease in the macrophage fusion on patterns compared to planar surface was observed on metallic glass pillars with diameters of 55, 100, and 150 nm [13] and titania nanotube with a diameter of 78 nm [15]. The nano-patterns restrict cell spreading and reduced the cytoskeletal remodeling, resulting in a decrease in the macrophage fusion [13]. Interestingly, Wang et al. reported that the metallic glass micro-pillar pattern with a diameter of 1 μm induced a greater macrophage fusion but nano-pillar with a diameter of 40 nm restricted the area of

macrophage fusion, nevertheless, the numbers of multinucleated cells were similar on both the patterns [14]. Therefore, adequate type and size of patterns are important for high efficacy of macrophage fusion on micro/nano-patterns. Our 1 µm or 500 nm pillar patterning of COP films increased the number of multinucleated cells generated by fusion of RAW 264.7 cells.

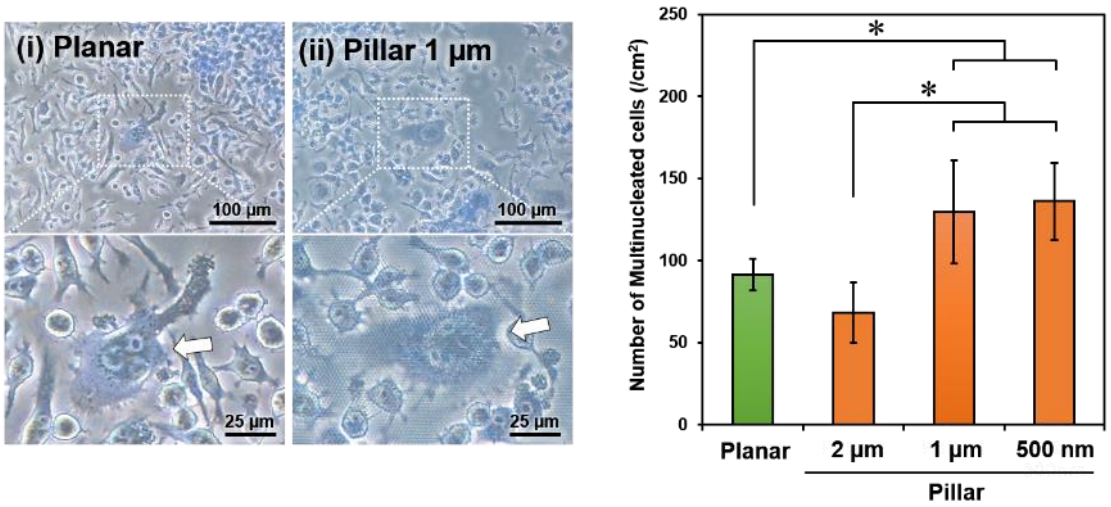

(a) *(b)*

*Fig 3. (a) Optical microscope images of RAW 264.7 cells on the COP pillar-patterned film after 6 days-culturing. The cells were observed (i) on the corresponding planar surface and (ii) on pillars with a diameter of 1 µm and a height of 500 nm. Dotted square area is magnified in the images below. White arrows indicate multinucleated cells. (b) Bar graph of the number of multinucleated cells generated by RAW 264.7 macrophage fusion on the pillars with diameters of 2 µm, 1 µm, and 500 nm and a height of 500 nm after 6 days-culturing. * indicates $p < 0.05$.*

Figure 4a shows SEM images of the representative morphology of multinucleated cells generated from RAW264.7 macrophages on COP pillar-patterned film after 6 days of culture. The multinucleated cells were observed as a large cell area and with flat shape on both the pillar patterns and planar surface. The cells exhibited various shapes and there was no significant difference in the cell shape and area amongst both the substrates (detailed data not shown). Interestingly, the filopodia of multinucleated cells on the pillar pattern seemed to grasp the edge of the pillar shape. Figure 4b shows characteristic bright field microscopy images of TRAP-staining multinucleated cells. Although TRAP is one of osteoclast marker enzymes, some

multinucleated macrophages exhibit positive TRAP staining [8, 18, 19]. TRAP activity of multinucleated macrophage was influenced by culture period [18], microstructures of hydroxyapatite, and plasma components [8]. Thus, we carried out TRAP staining for functional characterization of macrophages. Most of the multinucleated cells were TRAP-negative (Fig. 4b-iii). On the other hand, few multinucleated cells and mononuclear cells were TRAP-positive (Red-staining cells; Fig 4b-iv). The number of TRAP-positive cells may be less than one tenth of number of TRAP-negative cells in our culture condition (data not shown). The mononuclear or multinucleated macrophages would have functional diversities and change functions depending on environment in culture [4, 5, 28].

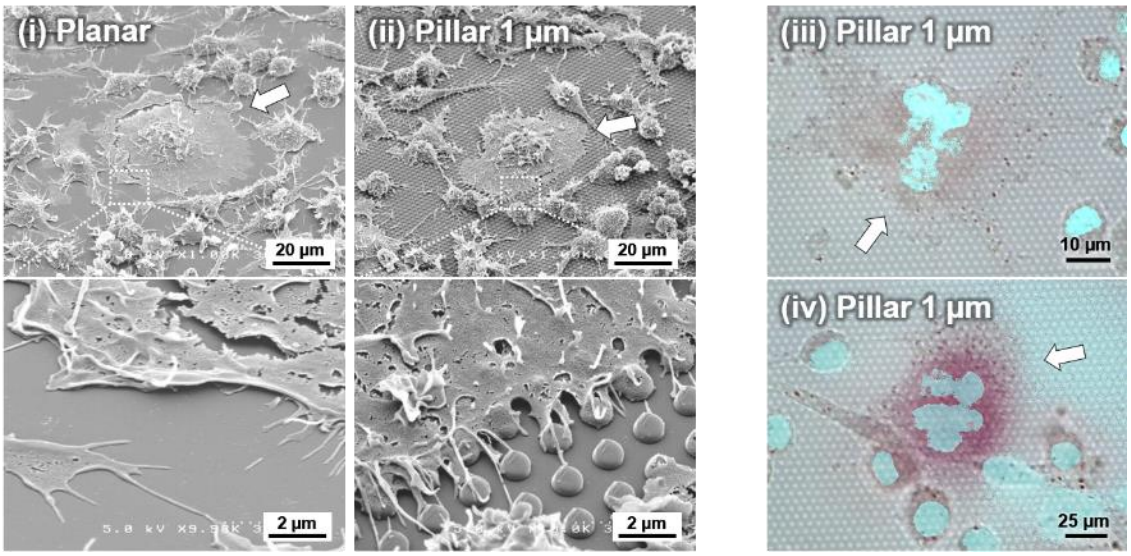

(a) *(b)*

Fig 4. Typical images of multinucleated cells generated by RAW 264.7 macrophage fusion on COP pillar-patterned film. The cells were cultured on the pillar-patterned film with a diameter of 1 µm and a height of 500 nm height for 6 days. (a) SEM images of the multinucleated cells on (i) planar surface and (ii) COP pillar pattern film at a 45 ° tilt angle. (b) Bright field and fluorescence microscopy images showing tartrate-resistant acid phosphatase (TRAP; red) staining. (iii) TRAP-negative cells and (iv) TRAP-positive cells. Nuclei were stained with DAPI and are shown in blue color. White arrows indicate multinucleated cells.

Figure 5 shows the immunofluorescence images of the RAW 264.7 macrophages cultured on pillar-pattern films with diameters of 2 µm, 1 µm, and 500 nm

and a height of 500 nm for 6 days. F-actin (red), vinculin (green), and nuclei (blue) in mononuclear cells (Fig. 5a) and multinucleated cells (Fig. 5b) were stained. Expression of F-actin and vinculin in mononuclear cells on planar surface was weak. Interestingly, F-actin and vinculin were expressed relatively strong in the cells on pillars and were localized along the circumference of the pillar as observed from the top view. The diameter of each ring corresponded to the diameter of 2 μm, 1 μm, or 500 nm pillars, respectively. The unique ring-shaped expression shape on the pillar pattern is similar to ring expression of F-actin dots of RAW 264.7 cells on ovalbumin-stamped square-pattern with 4 μm sides and 5 nm height [29]. The ring-shaped expression of F-actin and vinculin in mononuclear cells on pillars represents "frustrated phagocytosis". Thus, frustrated phagocytosis in macrophage on the pillar pattern contributes to the increased macrophage fusion. Expression pattern of F-actin and vinculin in multinucleated cells was also similar to that observed for mononuclear cells (Fig. 5b). Expression on pillars was comparatively stronger than that on planar surface. Although the ring-shaped expression of F-actin and vinculin was observed in multinucleated cells on pillars, ring shape was only observed in the local area of multinucleated cells. However, actin ring or podosome belt of macrophages [19] could not be observed in this study. In the future, we shall try to determine the formation of actin ring or podosome belt in multinucleated cells after longer culture periods.

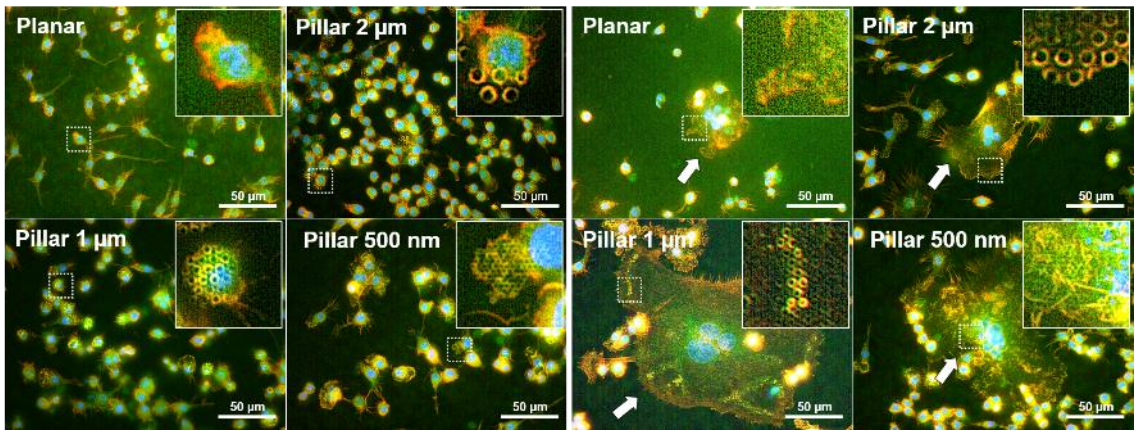

(a) *(b)*

Fig 5. Immunofluorescence images of (a) mononuclear cells and (b) multinucleated cells when RAW 264.7 cells were cultured on COP pillar-pattern films with diameters of 2 μm, 1 μm, and 500 nm and a height of 500 nm for 6 days. Red = F-actin; green = vinculin; blue = nuclei. White arrows indicate the multinucleated cells. Dotted square area in each image is magnified and shown in the inset.

4. Conclusions

We prepared COP pillar-patterned film with diameters of 2 μm, 1 μm, and 500 nm and a height of 500 nm via nanoimprinting and investigated the effect of the pillar patterns on macrophage attachment and fusion using RAW264.7 cells. Our results suggest that the cell attachment and macrophage fusion were improved by pillar patterning with diameters of 1 μm and 500 nm ($p < 0.05$). The mononuclear and multinucleated cells on the pillar pattern seem to grasp the pillars as observed in SEM images. Interestingly, the expression of F-actin and vinculin in mononuclear and multinucleated cells on the pillar patterns appeared, under fluorescence microscope, along the circumference of the pillar in the form of a ring, indicating "frustrated phagocytosis". Thus, frustrated phagocytosis in macrophages for pillars contributes to increased fusion depending on the size of the pillars. The detailed reason for increased fusion needs to be determined. Further studies about macrophage fusion on several different types of fine micro/nano-patterns are also required.

Acknowledgments

This study was funded by JSPS KAKENHI Grant Number (JP25463047 and JP16K11822), Suzuken Memorial Foundation, and "Building of Consortia for the Development of Human Resources in Science and Technology" through Ministry of Education, Culture, Sports, Science and Technology, Japan. We would like to thank Editage (www.editage.jp) for English language editing.

References

[1] D. M. Dohan Ehrenfest, P. G. Coelho, B. S. Kang, Y. T. Sul, T. Albrektsson, Trends Biotechnol. **28**, 198 (2010).
[2] C. N. Elias, F. A. Rocha, A. L. Nascimento, P. G. Coelho, J. Mech. Behav. Biomed. Mater. **16**, 169 (2012).
[3] D. M. Brunette, Int. J. Oral Maxillofac. Implants **3**, 231 (1988).
[4] Z. Sheikh, P. J. Brooks, O. Barzilay, N. Fine, M. Glogauer, Materials **8**, 5671 (2015).
[5] R. J. Miron, H. Zohdi, M. Fujioka-Kobayashi, D. D. Bosshardt, Acta Biomater. **46**,

15 (2016).
[6] A. Rich, A. K. Harris, J. Cell Sci., **50**, 1 (1981).
[7] T. N. Salthouse, J. Biomed. Mater. Res. **18**, 395 (1984).
[8] K. Morishita, E. Tatsukawa, Y. Shibata, F. Suehiro, M. Kamitakahara, T. Yokoi, K. Ioku, M. Umeda, M. Nishimura, T. Ikeda, Acta Biomater. **39**, 180 (2016).
[9] N. L. Davison, B. ten Harkel, T. Schoenmaker, X. Luo, H. Yuan, V. Everts, F. Barrère-de Groot, J. D. de Bruijn, Biomaterials **35**, 7441 (2014).
[10] H. Moon, C. V. Cremmel, A. Kulpa, N. A. Jaeger, R. Kappelhoff, C. M. Overall, J. D. Waterfield, D. M. Brunette, J. Biomed. Mater. Res. A **104**, 2243 (2016).
[11] E. Lamers, X. F. Walboomers, M. Domanski, L. Prodanov, J. Melis, R. Luttge, L. Winnubst, J. M. Anderson, H. J. Gardeniers, J. A. Jansen, Nanomedicine **8**, 308 (2012).
[12] S. Chen, J. A. Jones, Y. Xu, H. Y. Low, J. M. Anderson, K. W. Leong, Biomaterials **31**, 3479 (2010).
[13] J. Padmanabhan, M. J. Augelli, B. Cheung, E. R. Kinser, B. Cleary, P. Kumar, R. Wang, A. J. Sawyer, R. Li, U. D. Schwarz, J. Schroers, T. R. Kyriakides, Sci. Rep. **6**, 33277 (2016).
[14] J. Wang, A. M. Loye, J. Ketkaew, J. Schroers, T. R. Kyriakides, ACS Appl. Bio. Mater. **1**, 51 (2018).
[15] P. Neacsu, A. Mazare, A. Cimpean, J. Park, M. Costache, P. Schmuki, I. Demetrescu, Int. J. Biochem. Cell Biol. **55**, 187 (2014).
[16] T. Akasaka, H. Miyaji, T. Imamura, N. Kaga, A. Yokoyama, Y. Yoshida, Dig. J. Nanomater. Bios. **12**, 281 (2017).
[17] R. Takata, T. Akasaka, M. Tamai, Y. Yoshimura, T. Taira, H. Miyaji, Y. Tagawa, S. Yamagata, J. Iida, Y. Yoshida, Dig. J. Nanomater. Bios. **13**, 451 (2018).
[18] U. A. Khan, S. M. Hashimi, M. M. Bakr, M. R. Forwood, N. A. Morrison, J. Cell Biochem. **114**, 1772 (2013).
[19] B. ten Harkel, T. Schoenmaker, D. I. Picavet, N. L. Davison, T. J. de Vries, V. Everts, PLoS One **10**, e0139564 (2015).
[20] N. Kaga, T. Akasaka, R. Horiuchi, Y. Yoshida, A. Yokoyama, Nano Biomed. **8**, 74 (2016).
[21] R. Makita, T. Akasaka, S. Tamagawa, Y. Yoshida, S. Miyata, H. Miyaji, T. Sugaya, Beilstein J. Nanotechnol. **9**, 1735 (2018).
[22] M. Yamazaki, J. Mol. Catal. **213**, 81 (2004).
[23] C. Strehmel, H. Perez-Hernandez, Z. Zhang, A. Löbus, A. F. Lasagni, M. C. Lensen, ACS Biomater. Sci. Eng. **1**, 747 (2015).

[24] E. W. Young, E. Berthier, D. J. Beebe, Anal. Chem. **85**, 44 (2013).

[25] C. Alvim Valente, P. Cesar Chagastelles, N. Fontana Nicoletti, G. Ramos Garcez, B. Sgarioni, F. Herrmann, G. Pesenatto, E. Goldani, M. L. Zanini, M. M. Campos, R. Meurer Papaléo, J. Braga da Silva, N. R. de Souza Basso, J. Biomed. Mater. Res. A. **106**, 1522 (2018).

[26] B. Wójciak-Stothard, A. Curtis, W. Monaghan, K. MacDonald, C. Wilkinson, Exp. Cell. Res. **223**, 426 (1996).

[27] M. L. Lastra, M. S. Molinuevo, I. Blaszczyk-Lezak, C. Mijangos, M. S. Cortizo. J. Biomed. Mater. Res. A. 106, 570 (2018).

[28] J. M. Anderson, A. Rodriguez, D. T. Chang, Semin. Immunol. **20**, 86 (2008).

[29] A. M. Labrousse, E. Meunier, J. Record, A. Labernadie, A. Beduer, C. Vieu, T. Ben Safta, I. Maridonneau-Parini, Front. Immunol. **2**, 51 (2011).